RI 9480

REPORT OF INVESTIGATIONS/1993

Impact of Air Velocity on the Development and Detection of Small Coal Fires

By Margaret R. Egan

UNITED STATES DEPARTMENT OF THE INTERIOR

BUREAU OF MINES

U.S. Department of the Interior
Mission Statement

As the Nation's principal conservation agency, the Department of the Interior has responsibility for most of our nationally-owned public lands and natural resources. This includes fostering sound use of our land and water resources; protecting our fish, wildlife, and biological diversity; preserving the environmental and cultural values of our national parks and historical places; and providing for the enjoyment of life through outdoor recreation. The Department assesses our energy and mineral resources and works to ensure that their development is in the best interests of all our people by encouraging stewardship and citizen participation in their care. The Department also has a major responsibility for American Indian reservation communities and for people who live in island territories under U.S. administration.

Report of Investigations 9480

Impact of Air Velocity on the Development and Detection of Small Coal Fires

By Margaret R. Egan

UNITED STATES DEPARTMENT OF THE INTERIOR
Bruce Babbitt, Secretary

BUREAU OF MINES

Library of Congress Cataloging in Publication Data:

Egan, Margaret R.

Impact of air velocity on the development and detection of small coal fires / by Margaret R. Egan.

p. cm. — (Report of investigations; 9480)

Includes bibliographical references (p. 15).

Supt. of Docs. no.: I 28.23:9480.

1. Mine fires. 2. Mine ventilation. 3. Coal mines and mining—Fires and fire prevention. I. Title. II. Series: Report of investigations (United States. Bureau of Mines); 9480.

TN23.U43 [TN315] 622 s—dc20 [622'.82] 93-28787 CIP

CONTENTS

ILLUSTRATIONS

TABLES

UNIT OF MEASURE ABBREVIATIONS USED IN THIS REPORT

Btu/lb	British thermal unit per pound	mg/cm^3	milligram per cubic centimeter
°C	degree Celsius	mg/m^3	milligram per cubic meter
cm	centimeter	min	minute
cm^3	cubic centimeter	μm	micrometer
g/cm^3	gram per cubic centimeter	m/s	meter per second
g/g	gram per gram	$(m^2/s)/kW$	square meter per second per kilowatt
g/kJ	gram per kilojoule	m^3/s	cubic meter per second
$g/(m^3 \cdot ppm)$	gram per cubic meter times part per million	p/cm^3	particle per cubic centimeter
g/s	gram per second	p/kJ	particle per kilojoule
kg	kilogram	ppm	part per million
kJ/g	kilojoule per gram	$(ppm \cdot m^3)/kJ$	part per million times cubic meter per kilojoule
kW	kilowatt	p/s	particle per second
kW/min	kilowatt per minute	s	second
m	meter	V	volt
m^{-1}	reciprocal meter		

IMPACT OF AIR VELOCITY ON THE DEVELOPMENT AND DETECTION OF SMALL COAL FIRES

By Margaret R. Egan[1]

ABSTRACT

The U.S. Bureau of Mines conducted experiments in the intermediate-scale fire tunnel to assess the influence of air velocity on the gas production and smoke characteristics during smoldering and flaming combustion of Pittsburgh seam coal and its impact on the detection of the combustion products. On-line determinations of mass and number of smoke particles, light transmission, and various gas concentrations were made. From these experimental values, generation rates, heat-release rates, production constants, particle sizes, obscuration rates, and optical densities were calculated.

Ventilation has a direct effect on fire detection and development. The results indicate that, in general, increased air velocity lengthened the onset of smoke and flaming ignition, increased the fire intensity, but decreased the gas and smoke concentrations. Increased air velocity also lengthened the response times of all the fire sensors tested. Rapid and reliable detector response at this most crucial stage of fire development can increase the possibility that appropriate miner response (fire suppression tactics or evacuation) can be completed before toxic smoke spreads throughout the mine.

[1]Research chemist, Pittsburgh Research Center, U.S. Bureau of Mines, Pittsburgh, PA.

INTRODUCTION

The U.S. Bureau of Mines is currently studying the combustion process to better understand the basic elements of fire dynamics and to devise practical approaches to fire detection, prevention, and suppression. This research simulates a fire scenario involving an overheated conveyor belt roller that ignites loose coal, thereby releasing smoke and toxic gas into the mine's ventilation system. This report focuses on the critical time between the onset of a fire and its detection; in this interval the fire intensity can grow from smoldering to flaming in a matter of minutes.

Experiments were conducted in the intermediate-scale fire tunnel at air velocities of 0.57, 1.41, 2.64, and 3.66 m/s. The tunnel is instrumented with gas and smoke analyzers as well as a data collection system that can simultaneously calculate and record all instrument channels. The source of heat for the experiments was a 0.1-m-diameter cylindrical tube containing four strip heaters that was constructed to simulate an overheated conveyor belt roller.

Gas concentrations of carbon monoxide (CO), carbon dioxide (CO_2), hydrogen sulfide (H_2S), and sulfur dioxide (SO_2) were measured. From these values, gas ratios, fire intensities, generation rates, and gas production constants were calculated. Smoke characteristics, such as mass and number concentration, particle size, and optical density, were studied. In addition, the response of three types of fire sensors—CO, smoke, and the USBM-developed diesel-discriminating detector (DDD)—were tested. The DDD was designed to discriminate between smoke produced by a fire and the smoke produced by a diesel engine (*1*)[2].

The objectives of this study were as follows: (1) to analyze the gas production and smoke characteristics of both smoldering and flaming coal as a function of the air velocity, (2) to determine the effect air velocity has on ignition times, production rates, and detectability, and (3) to compare the response of the DDD to measured CO and smoke levels.

The detectability of a developing fire depends not only upon the concentration of CO or smoke produced, but also upon the rates at which they are produced. These rates depend upon the air velocity (via the fire growth rate and dilution). The data obtained here can be used to assist in defining the detectability of small coal fires using conventional CO or smoke sensors and the USBM's DDD.

MATERIALS AND EQUIPMENT

The test apparatus for these experiments included the USBM's intermediate-scale fire tunnel, Pittsburgh Seam coal, heating element, and gas and smoke analyzers. Each will be described in some detail. Prior to each experiment, gas calibrations and background readings were recorded. All instruments were continuously scanned and recorded throughout the experiment. A computer program was developed to process the collected data.

INTERMEDIATE-SCALE FIRE TUNNEL

In order to evaluate the effect that air velocity has on combustion emissions, the intermediate-scale fire tunnel at the USBM's Pittsburgh Research Center was adapted to provide a range of airflows. A schematic diagram shown in figure 1 presents an overview of the tunnel and its data-acquisition system. The first horizontal section of the tunnel measures 1.5 m in length and can be lifted to allow entrance for the placement of the coal and ignition source. The section begins with an air-intake cylinder that measures 0.25 m long by 0.3 m in diameter and gradually enlarges until it matches the tunnel dimensions at the hinged area. The fire zone measures 0.8 m wide by 0.42 m high by 1.22 m long. The fire zone is instrumented with thermocouples and flow probes and contains the coal pile with the heating element embedded in it. The remainder of the horizontal section measures 0.8 m wide by 0.8 m high by 8.78 m long. The diffusing grid begins the vertical section of the tunnel. Located in this section is an orifice plate that can be manually adjusted to attain the desired airflow. The final section is horizontal and ends at an exterior exhaust fan.

HEATING ELEMENT

A cylindrical heating element containing four strip heaters was used to simulate an overheated idler. A schematic of this heating element is shown in figure 2. The heating element is capable of reaching 500° C.

[2]Italic numbers in parentheses refer to items in the list of references preceding the appendix at the end of this report.

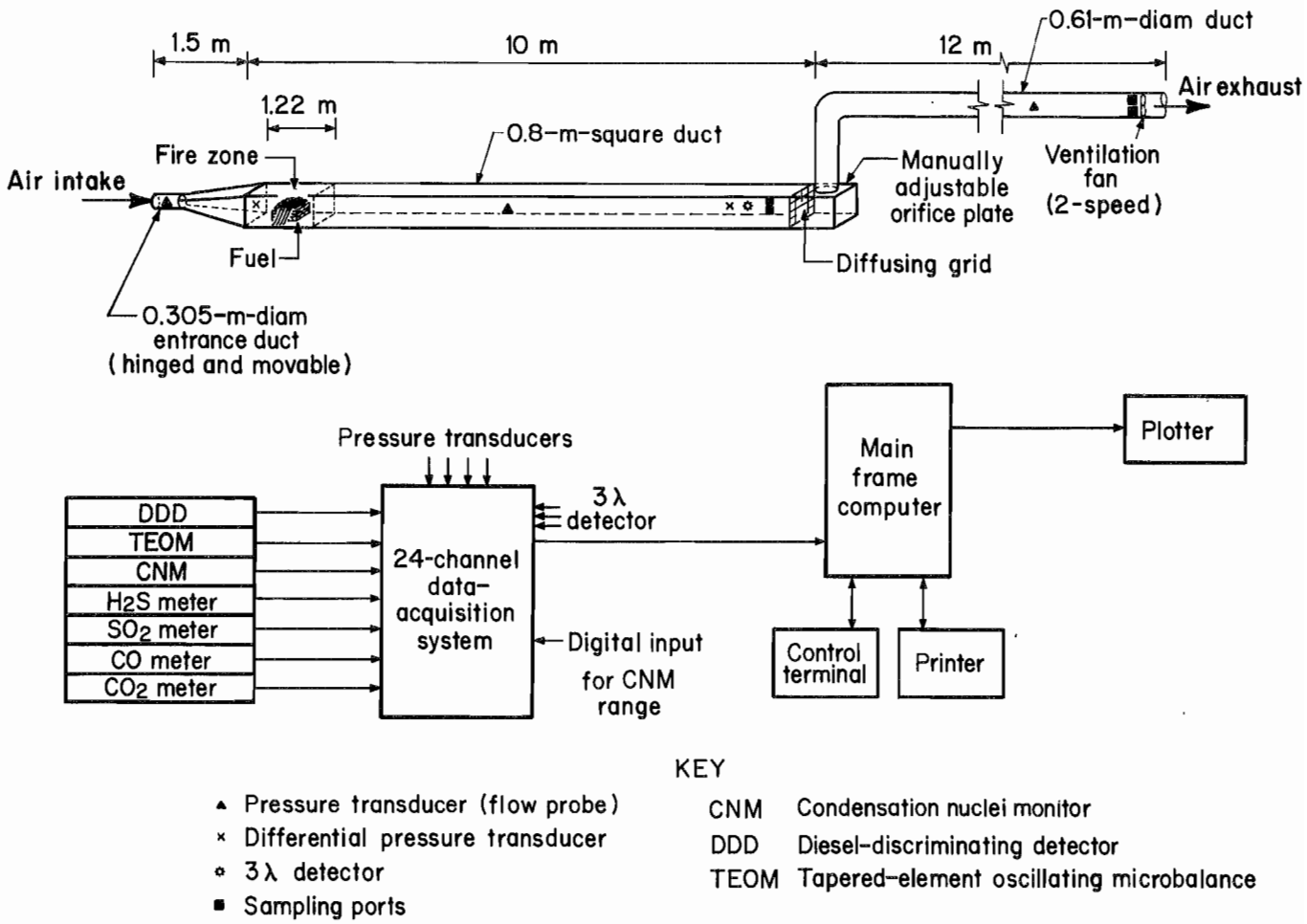

Figure 1.—Schematic of intermediate-scale tunnel (top) and data-acquisition system (bottom).

COAL PROPERTIES

Coal is a familiar substance but it has no fixed chemical formula. It was formed from decomposing plant material that was subjected to increased temperature and pressure for a prolonged period of time. The composition of the coal is, therefore, dependent upon the composition of the original plant material and the geologic processes to which it was subjected. However, all coals have carbon, hydrogen, and oxygen as major elements, with sulfur and nitrogen as minor elements. High volatile A bituminous coal from the Pittsburgh Coalbed was used for these 12 experiments. Its ultimate analysis revealed C 78%, H 5.3%, O 8.2%, N 1.6%, and S 1.3%. The proximate analysis showed moisture content 1.7%, ash content 5.6%, volatile matter 38.8%, and fixed C 53.9%. The heating value was 13,947 Btu/lb.

FLOW PROBES AND PRESSURE TRANSDUCERS

The ventilation through the tunnel is continuously measured using a bidirectional flow probe (*2*) in conjunction with a pressure transducer. The airflow produced by the exhaust ventilation is detected by the flow probe and converted to a linear electrical signal by the pressure transducer. This signal is then scanned and recorded by the data collection system. The locations of all the flow probes are also shown in figure 1. The flow probe used to obtain the velocity measurements is the one centered in the air-intake cylinder. The airflow over the coal pile was indirectly proportional to the air space and varied depending on the configuration of the mounded coal.

The stated accuracy of the flow probe is ±7%. The pressure transducer adds a maximum error of ±5.3%. Assuming the error to be accumulative, the maximum

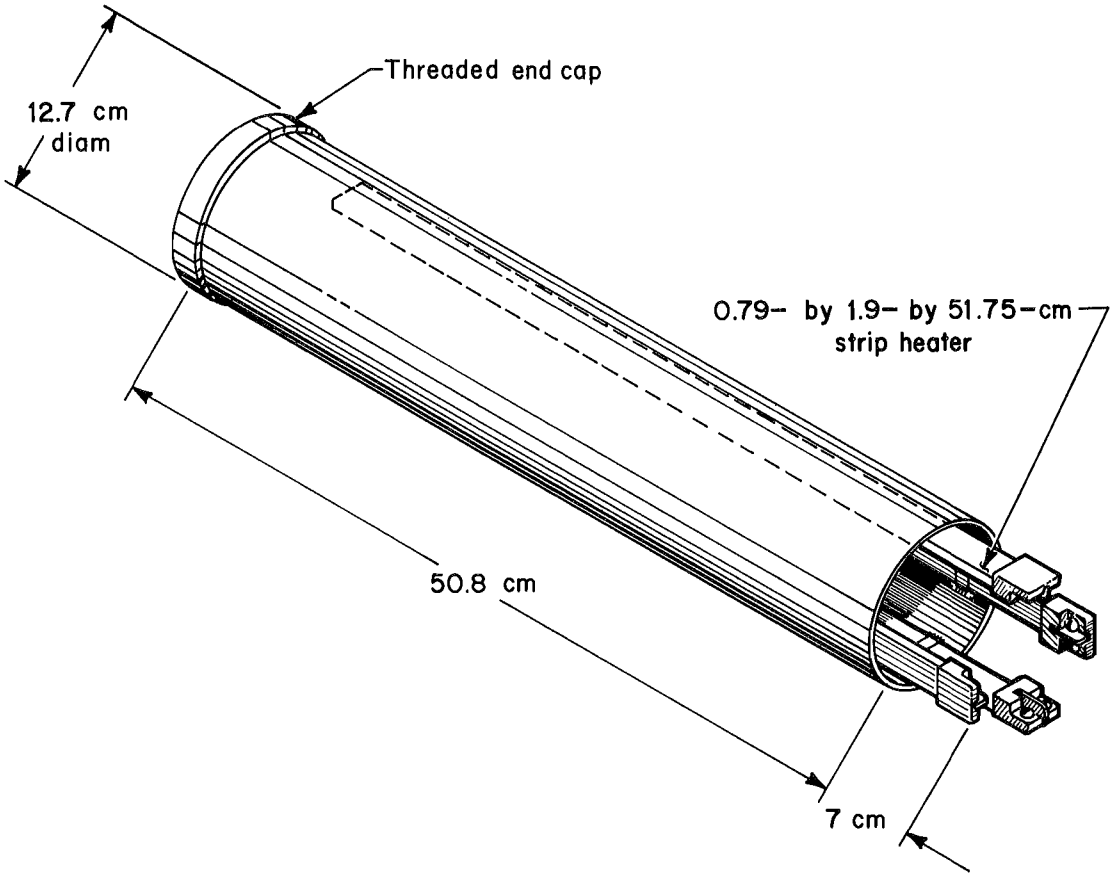

Figure 2.—Schematic of heating element.

velocity error for one data point is estimated to be ±12.3%. Averaging over 10 data points improves the accuracy by the square root of 10, resulting in the total estimated error of ±3.9% for the average data presented.

Additional velocity readings were made with a vane-type anemometer. This was done before each experiment to ensure that the tunnel adjustment was accurate.

GAS MONITORS

The two most abundant combustion emission gases measured were CO_2 and CO. The CO_2 analyzer measures accurately within 1% of full range or ±250 ppm. The CO analyzer measures accurately within 1% of full range or ±5 ppm.

As coal smolders, other gaseous volatiles containing nitrogen and sulfur can be formed, depending on the original composition of the coal. In this study, H_2S and SO_2 were measured continuously throughout the experiments. The H_2S analyzer measures accurately within 1% of full range or ±2.5 ppm. The SO_2 analyzer measures accurately within 1% of full range or ±0.5 ppm. All these gas analyzers had internal pumps and were calibrated at the beginning of each experiment.

SMOKE MONITORS

Condensation Nuclei Monitor

The number concentration in particles per cubic centimeter (N_o) was obtained with a Condensation Nuclei Monitor (CNM),[3] manufactured by Environment One Corp. It measures the concentration of submicrometer airborne particles (p) using a cloud chamber. The particulate cloud attenuates a light beam, which ultimately produces a measurable electrical signal. The accuracy is stated as ±20% of a point above 30% of scale on the

[3]Reference to specific products does not imply endorsement by the U.S. Bureau of Mines.

linear ranges, 3,000 to 300,000 p/cm³. In these experiments, this calculated error could be ±18,000 p/cm³.

In order to reduce the particulate count to within the range of the CNM, a 10% dilution of the smoke was necessary. Two flow meters, with a stated accuracy of ±2%, were used. One measured the flow of the sample and the other measured filtered room air. The dilution error was calculated to be from -15.2% to +22%. Over 10 data points, this error was reduced to ±7%. Adding this error to the already stated error of the instrument increases the total error to ±27%, making this the least accurate of all the instruments.

Tapered-Element Oscillating Microbalance

The mass concentration in milligrams per cubic meter (M_o) was obtained by a tapered-element oscillating microbalance (TEOM), developed by Rupprecht & Patashnick Co., Inc. (*3*). It measures the mass directly by depositing the particles on a filter attached to an oscillating tapered element. The oscillating frequency of the tapered element decreases as the deposited mass increases. The apparatus is capable of measuring the particulate concentration with better than 5% accuracy at the level used. The filter is specified to collect at least 50% of all particles with a volume mean diameter of 0.05 μm, with increasing collection efficiency as the diameter increases. Actual data obtained by the USBM using particles of volume mean diameter equal to 0.048 μm indicate a collection efficiency closer to 90%.

Since the diameter of average mass is calculated from the mass and number concentrations, its accuracy is dependent upon the precision of the TEOM and CNM. Considering these possible errors, the diameter of average mass may be off by a factor of ±3%.

Three-Wavelength Smoke Sensor

A three-wavelength light transmission technique developed by the USBM (*4*) was used to measure smoke concentration and obscuration. White light was transmitted through a smoke cloud to the detector. The beam was split into three parts, and each passed through an interference filter centered at wavelengths of 0.45, 0.63, or 1.00 μm. Each photodiode output was amplified and recorded as a linear electric signal.

Diesel-Discriminating Detector

The Bureau developed the DDD to distinguish between the emissions from diesel engines and fire smoke. The DDD's design is based on the fact that internal combustion engines generate particulates at much higher temperatures than can be found in most fires. The number of fire smoke particles increases when heated to 300° C, but particulates from internal combustion engines do not. A submicrometer-particle detector developed by the USBM was fitted with a dual-input ionization chamber. One portion of the smoke passes around a ceramic rod heated by a nichrome wire. The remaining portion of the smoke is unheated. A comparison is made between the number of particles from the heated and the unheated smoke. If only smoke from an internal combustion engine is present, the output signals cancel each other and no alarm is triggered. If only fire smoke is present, the signal from the heated sample is higher than the signal of the unheated sample. An imbalance of 0.025 V can trigger an alarm. When both fire smoke and diesel exhaust are present, an alarm is also triggered because the signal components associated with the engine smoke are canceled, but the fire smoke signals remain.

EXPERIMENTAL METHODS

Approximately 9 kg of coal was broken into pieces measuring 125 cm³ or less and was piled on and around the simulated roller. From 5 to 7.5 cm of coal rested on top of the roller, producing a pile of coal approximately 18 cm high and 27 cm wide at its base. The timing of all experiments began when the heating element was turned on. The power was set at 150 V for 15 min then raised to 200 V. Thirty minutes after flaming combustion was sighted, the power was turned off. The coal continued to sustain flaming combustion. Each experiment lasted approximately 95 min.

Twelve experiments with Pittsburgh Seam coal were completed, three at each air velocity (V_o), calculated over the coal pile. These resulted in a ventilation rate (V_oA_o) of 0.12, 0.30, 0.55, and 0.77 m³/s. An anemometer was used to determine the velocity at the air-intake cone.

CALCULATIONS

It is necessary to measure certain parameters in order to compare the steady-state combustion products and ultimately the hazards of various fuels. Among these measurements are gas concentrations, smoke particle mass and number concentrations, ventilation rate, and obscuration rate. Other combustion properties can be calculated once these values are known.

PRODUCT GENERATION RATES

In a ventilated system, the generation rate ($\dot{G}_X$) of a product is related to the bulk average concentration increase above ambient (ΔX) by the expression

$$\dot{G}_X = M_X(V_oA_o)(\Delta X), \quad (1)$$

where $M_{CO} = 1.25 \times 10^{-3}$ g/(m^3•ppm),

$M_{CO_2} = 1.97 \times 10^{-3}$ g/(m^3•ppm),

$M_{H_2S} = 1.52 \times 10^{-3}$ g/(m^3•ppm),

$M_{SO_2} = 2.86 \times 10^{-3}$ g/(m^3•ppm),

V_oA_o = ventilation rate, m^3/s,

and ΔX = measured change in a given quantity.

HEAT-RELEASE RATES

It has been shown (*5*) that the actual heat-release rate realized during a fire can be calculated from the generation rates of CO and CO_2 by the following expression:

$$\dot{Q}_A = \left[\frac{H_C}{K_{CO_2}}\right]\dot{G}_{CO_2} + \left[\frac{H_C - H_{CO}(K_{CO})}{K_{CO}}\right]\dot{G}_{CO}, \quad (2)$$

where $\dot{Q}_A$ = actual heat release, kW,

H_C = net heat of complete combustion of coal, 31.0 kJ/g,

H_{CO} = heat of combustion of CO, 10.1 kJ/g,

K_{CO_2} = stoichiometric yield of CO_2, 2.86 g/g.

and K_{CO} = stoichiometric yield of CO, 1.82 g/g.

Substituting the values in equations 1 and 2 yields

$$\dot{Q}_A = V_oA_o[(0.0214)(\Delta CO_2) + 8.5 \times 10^{-3}(\Delta CO)]. \quad (3)$$

Since measurements of V_oA_o, ΔCO_2, and ΔCO were made continuously, the actual heat-release rates could be calculated using equation 3. Since heat is generated only in those reactions where CO and CO_2 are produced (*5*), and CO and CO_2 are the main products of combustion, this calculation can also be used to determine fire intensity.

PRODUCTION CONSTANTS

In an actual mine fire, it is often difficult, if not impossible, to calculate the actual heat of combustion. Moreover, since the true yield of a combustion product depends upon this information, significant errors can result in predicting the resultant concentration increases. For flaming fires, the relative hazards tend to increase with the actual heat-release rate that results.

For this reason, production constants or beta values (β_X) can be calculated for a given product by the expression

$$\beta_X = \frac{\dot{G}_X}{\dot{Q}_A}. \quad (4)$$

Using the rate of formation of gas or smoke as a function of the fire size is also beneficial in comparing the combustion hazards of different fuels.

In the initial stages of fire development, an important parameter is the fire growth rate. This can be calculated from the heat-release rate by the following expression:

$$\dot{Q}_{fg} = \frac{\dot{Q}_p - \dot{Q}_i}{t_p - t_i}, \quad (5)$$

where $\dot{Q}_{fg}$ = fire growth rate, kW/min,

$\dot{Q}_p$ = peak heat-release rate, kW,

$\dot{Q}_i$ = heat-release rate at ignition, kW,

t_p = time of peak heat release, min,

and t_i = time of ignition, min.

SMOKE INTENSITY PARAMETERS

There are several methods by which smoke intensity can be measured. The transmission of light through smoke (T) can be measured using the three-wavelength smoke detector. Some factors influencing T are the number, size, and refractive index of the particles, and light frequency. T is calculated from the expression

$$T = \frac{I_S - I_O}{I - I_O}, \quad (6)$$

where I_S = intensity of light in the presence of smoke,

I = intensity of light in the absence of smoke,

and I_O = background reading in the absence of light.

A convenient measurement of smoke density is to examine the obscurant effect of smoke. It is calculated from the expression

$$\% \text{ obscuration} = \frac{(I - I_O) - (I_S - I_O)}{I - I_O}(100). \quad (7)$$

Smoke evolution is most often expressed in terms of D (optical density per unit path length) because it correlates with visibility. D is related to T by the following expression:

$$D = -\frac{1}{\ell}(\log T), \quad (8)$$

where ℓ = path length, m.

D becomes a convenient measure of fire hazard and deductibility, because escape and rescue are dependent upon visibility. Most smoke detectors are triggered at a D of 0.044 m^{-1} or less. The probability of escape and rescue is reduced significantly once the critical level of smoke (D = 0.218 m^{-1}) has accumulated (*6*). The obscuration and D values presented in this report are an average of the attenuation of the beam of light at the two wavelengths in the visible range, 0.45 and 0.63 μm.

SMOKE PARTICLE DIAMETERS

The size of the smoke particles can also be determined using the three-wavelength smoke detector. The extinction-coefficient ratio can be calculated for each pair of wavelengths (λ) from the following log-transmission ratios:

$$\frac{\ln T_{\lambda=1.00}}{\ln T_{\lambda=0.63}}, \quad \frac{\ln T_{\lambda=1.00}}{\ln T_{\lambda=0.45}}, \quad \text{or} \quad \frac{\ln T_{\lambda=0.63}}{\ln T_{\lambda=0.45}}.$$

Using these extinction coefficients and the curve in reference 4, figure 11, the volume-to-surface mean particle diameter (d_{32}) can be determined. (Calculation of the extinction-coefficient curves assumes spherical particles with an estimated refractive index.) The T must be less than 0.85 before reliable particle sizes can be calculated using this technique.

Measurements of both M_o and N_o of the smoke can be used to calculate the average size of the smoke particles, using the expression

$$\frac{\pi d_m^3}{6}(\rho_p)(N_o) = 1 \times 10^3 \, M_o, \quad (9)$$

where ρ_p = individual particle density, g/cm^3,

d_m = diameter of a particle of average mass, μm,

M_o = mass concentration, mg/m^3,

and N_o = number concentration, p/cm^3.

Assuming a value of ρ_p = 1.1 g/cm^3 (*7*), then the diameter of average mass (d_m) can be calculated in micrometers from

$$d_m = 12.02 \left[\frac{M_o}{N_o}\right]^{1/3}. \quad (10)$$

SMOLDERING COAL RESULTS AND DISCUSSION

All the smoldering values listed in this report are an average of concentrations between the first indication of smoke and flaming ignition. Table 1 lists the air velocity (V_o) and combustion stage. The fires at the highest air velocity had the latest onset of smoldering. The onset of smoldering (t_s) was measured from the increase in N_o as detected by the CNM and did not depend exclusively on visual observation. Ignition or sustained flaming (t_i) was easier to observe although it also coincided with a marked increase in the N_o.

SMOLDERING COAL GAS CONCENTRATIONS AND HEAT PRODUCTION

Table 2 lists the gas concentrations and ratios for smoldering coal. The results of test 8 showed an abnormally high CO_2 level considering the test parameters for that sequence of tests. It was regarded as an instrument malfunction and not reported or used in calculations. The results indicate that all gas concentrations decreased as the air velocity increased. At the higher velocities (tests 7 through 12), the concentrations of the gases are too low to give reliable ratios. However, the gas ratios in tests 1 through 6 increased as the air velocity increased.

Table 3 lists the generation, heat-release, and fire growth rates for smoldering coal. The generation rates tended to decrease as the air velocity increased. The fire intensity, as measured by the heat-release rate, also decreased with air velocity.

Table 1.—Combustion stage times at four airflows

Test	t_s, min	t_i, min	t_i-t_s, min
V_o, 0.57 m/s			
4	17	36.0	19.0
5	17	35.5	18.5
6	17	38.0	21.0
Av	17	36.5	19.5
V_o, 1.41 m/s			
1	16	31.0	15.0
2	17	35.0	18.0
3	17	35.0	18.0
Av	17	33.7	17.0
V_o, 2.64 m/s			
7	21	43.0	22.0
8	21	48.0	27.0
9	21	37.0	16.0
Av	21	42.7	21.7
V_o, 3.66 m/s			
10	26	35.0	9.0
11	21	34.5	13.5
12	25	40.0	15.0
Av	24	36.5	12.5

Table 2.—Smoldering coal gas concentrations and ratios at four airflows

Test	CO_2, ppm	CO, ppm	SO_2, ppm	H_2S, ppm	Smoldering coal ratios		
					CO_2-CO	SO_2-CO	H_2S-CO
V_o, 0.57 m/s							
4	50	79	9	5	0.63	0.115	0.066
5	151	84	5	3	1.79	.059	.039
6	70	88	6	4	.79	.063	.048
Av	90	84	7	4	1.07	.079	.051
V_o, 1.41 m/s							
1	21	13	1	1	1.65	0.075	0.061
2	44	25	4	2	1.76	.160	.098
3	17	32	6	2	.52	.174	.064
Av	27	23	4	2	1.31	.136	.074
V_o, 2.64 m/s							
7	9	10	<1	0	0.87	0.037	ND
8	NR	11	1	1	ND	.077	0.082
9	19	13	2	1	1.45	.154	.112
Av	14	11	1	1	1.24	.089	.097
V_o, 3.66 m/s							
10	3	9	<1	0	0.38	0.044	ND
11	8	7	<1	0	1.24	.040	ND
12	5	10	<1	0	.54	.023	ND
Av	6	9	<1	0	.72	.036	ND

ND Not determined.
NR Not reported.

SMOLDERING COAL SMOKE CHARACTERISTICS

The initial observation of smoke was confirmed by an increase in the N_o. The smoke level rose rapidly during the smoldering stage. An average of the smoke characteristics during the smoldering stage can be found in table 4. The M_o and N_o tended to decrease with increased air velocity. The obscuration and D also decreased until the highest air velocity (tests 10 through 12), when the smoke levels were too low to reliably detect. The smoke-to-CO ratio seemed unaffected by velocity. The average value of D-CO for all the tests was 0.017. This is in reasonable agreement with a previously reported (*8*) value of 0.024.

FIRE DETECTION

A comparison of the alarm times for three types of fire sensors (measured from the start of each test) can be found in table 5. The two lower air velocities are listed because their smoke concentrations reached threshold levels. For each test, a span of less than 2 min separates the first alarm from the last. The CO sensor usually alarmed first. The smoke sensor and the DDD alarmed slightly later. The alarm times at the lower air velocity were shorter than those at the higher velocity.

The DDD alarm times compare favorably with those of the CO and smoke sensors. For this test comparison, the threshold levels were 5 ppm for CO sensors, 0.044 m^{-1} of D for smoke sensor, and 0.025 V for the DDD. On the average, only 49.2 s separated the time of the first sensor to reach its alarm threshold from the alarm time of the DDD. When the DDD alarmed, the CO level averaged 8.2 ppm and the smoke D level averaged 0.096 m^{-1}. Such response seems quite reasonable considering the function of the DDD is more than just smoke detection.

Table 3.—Smoldering coal generation and heat-release rates at four airflows

Test	$\dot{G}_{CO}$, 10^{-3} g/s	$\dot{G}_{CO_2}$, 10^{-2} g/s	$\dot{G}_{SO_2}$, 10^{-4} g/s	$\dot{G}_{H_2S}$, 10^{-4} g/s	$\dot{Q}_A$, 10^{-1} kW
			V_o, 0.57 m/s		
4	12.10	1.20	31.89	9.73	2.12
5	13.58	3.84	18.48	6.51	5.09
6	14.10	1.76	20.24	8.29	2.87
Av	13.26	2.26	23.37	8.18	3.36
			V_o, 1.41 m/s		
1	5.04	1.31	8.66	3.73	1.77
2	9.63	2.66	35.20	11.44	3.55
3	12.11	1.00	48.14	9.50	1.91
Av	8.93	1.66	30.67	8.22	2.41
			V_o, 2.64 m/s		
7	7.33	1.00	6.26	ND	1.59
8	7.50	ND	13.17	7.52	ND
9	9.47	2.16	33.35	12.88	2.99
Av	8.10	1.08	17.59	10.20	2.29
			V_o, 3.66 m/s		
10	8.44	0.50	8.60	ND	1.12
11	6.56	1.28	5.97	ND	1.84
12	9.61	.82	5.08	ND	1.54
Av	8.20	.87	6.55	ND	1.50

ND Not determined.

Table 4.—Smoldering coal smoke characteristics at four airflows

Test	M_o, mg/m^3	N_o, 10^5 p/cm^3	d_m, μm	d_{32}, μm	Obscuration, %	D, m^{-1}	D-CO ratio
			V_o, 0.57 m/s				
4	34.68	7.79	0.426	0.516	23.58	1.168	0.014
5	32.45	6.70	.438	.446	23.22	1.148	.014
6	37.99	7.63	.442	.499	24.13	1.200	.014
Av	35.04	7.37	.435	.487	23.65	1.172	.014
			V_o, 1.41 m/s				
1	17.64	10.49	0.308	0.338	8.81	0.401	0.032
2	11.68	9.26	.280	.385	13.53	.631	.025
3	ND	7.13	ND	.405	12.78	.594	.019
Av	14.66	8.96	.294	.376	11.71	.542	.025
			V_o, 2.64 m/s				
7	5.06	5.77	0.248	ND	3.21	0.142	0.014
8	8.43	5.19	.304	ND	3.03	.134	.013
9	10.55	4.91	.334	0.241	2.59	.114	.009
Av	8.01	5.29	.295	.241	2.94	.130	.012
			V_o, 3.66 m/s				
10	7.41	1.27	0.466	0.296	3.91	0.173	0.020
11	7.75	1.96	.409	ND	3.29	.145	.021
12	5.52	2.26	.349	ND	2.50	.110	.011
Av	6.89	1.83	.408	.296	3.23	.143	.017

ND Not determined.

Table 5.—Comparison of sensor alarm times,[1] minutes at two airflows

Test	CO	Smoke	DDD
	V_o, 0.57 m/s		
4	22.52	21.62	22.81
5	20.01	21.34	21.36
6	21.60	22.36	23.59
Av	21.38	21.77	22.59
	V_o, 1.41 m/s		
1	22.86	23.12	23.13
2	24.20	23.01	23.15
3	22.60	23.06	24.19
Av	23.22	23.06	23.49

[1]The alarm threshold levels are 5 ppm for a CO sensor, D equal to 0.044 m^{-1} for a smoke sensor, and 0.025 V for the DDD.

FLAMING COAL RESULTS AND DISCUSSION

The flaming coal results in tables 6 through 9 are an average of the last 5 min before the heater was turned off. This represented the most constant production of emissions while the combustion was being thermally driven. After the heating element was turned off, most emissions except CO began to decrease. CO slowly increased while the heating element was on then rapidly increased once it was turned off when combustion changed to a more incomplete mode.

FLAMING COAL GAS CONCENTRATIONS AND HEAT PRODUCTION

Table 6 lists the gas concentrations and ratios for flaming coal. All gas concentrations and ratios tended to decrease as the air velocity increased. This effect is better demonstrated at the lower velocities and is less evident at the highest velocity.

Table 7 lists the generation and the heat-release rates for flaming coal. The generation rates increased as the air velocity increased. The generation rates for SO_2 and H_2S from tests 10 through 12 are based on concentrations too low to yield reliable rates. The fire intensity, as measured by the heat-release rate, $\dot{Q}_A$, also increased with air velocity as more oxygen was supplied to the fire. $\dot{Q}_A$ is the average heat release as measured during the last 5 min of thermally-driven combustion. Table 8 shows the actual heat release, $\dot{Q}_i$, as measured at ignition, t_i, (table 1) and the peak heat release, $\dot{Q}_p$, as measured at t_p. The rate increases as the airflow increases, especially at the higher airflows. This is demonstrated in figure 3, which plots the fire intensity of a typical test at each air velocity. The results showed that the fire intensity increased nearly linearly from t_i to t_p. The fire growth rate, Q_{fg}, became steeper as the velocity increased. After the heating element was turned off, at about minute 66, flaming combustion continued but decreased in intensity.

FLAMING COAL SMOKE CHARACTERISTICS

Table 9 lists the smoke characteristics for flaming coal. The obscuration and D decreased as the air velocity increased. These smoke characteristics are influenced not only by the amount of smoke produced but also by its movement through the tunnel. The other smoke characteristics (M_o, N_o, and particle size) did not show any obvious trends with air velocity. The D-CO ratio remained fairly constant throughout all velocity ranges.

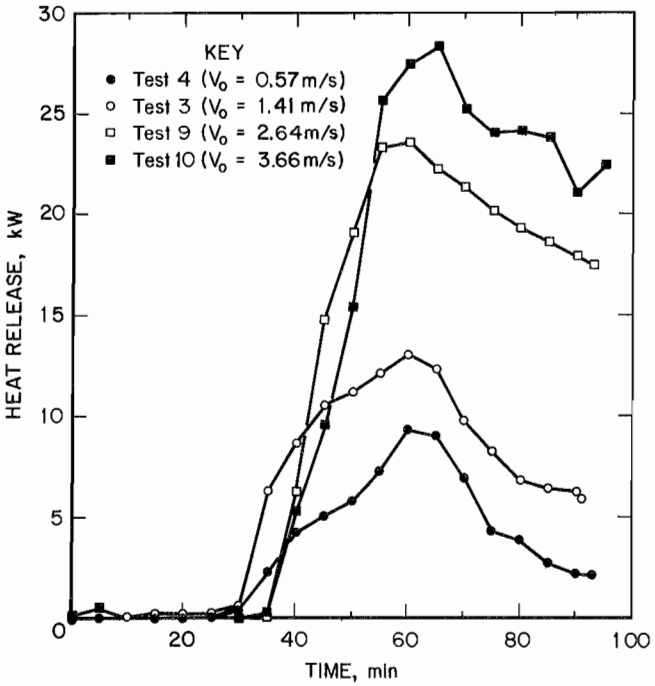

Figure 3.—Fire intensity versus time for a typical experiment at each air velocity.

Table 6.—Flaming coal gas concentrations and ratios at four airflows

Test	CO_2, ppm	CO, ppm	SO_2, ppm	H_2S, ppm	Flaming coal ratios		
					CO_2-CO	SO_2-CO	H_2S-CO
			V_o, 0.57 m/s				
4	2,495	216	95	18	11.55	0.44	0.08
5	3,659	184	52	17	19.93	.29	.09
6	3,169	213	41	15	14.89	.19	.07
Av	3,108	204	63	17	15.45	.31	.08
			V_o, 1.41 m/s				
1	1,302	126	48	ND	10.35	0.38	ND
2	1,517	96	77	12	15.76	.80	0.12
3	1,337	161	72	11	8.31	.45	.07
Av	1,386	128	66	11	11.47	.55	.09
			V_o, 2.64 m/s				
7	748	103	21	4	7.24	0.20	0.03
8	NR	135	26	10	NR	.19	.08
9	1,226	125	30	10	9.82	.24	.08
Av	987	121	25	8	8.53	.21	.06
			V_o, 3.66 m/s				
10	1,151	119	2	0	9.63	0.02	0
11	989	143	7	1	6.92	.05	<.01
12	1,496	149	6	1	10.02	.04	<.01
Av	1,212	137	5	1	8.86	.04	<.01

ND Not determined.
NR Not reported.

Table 7.—Flaming coal generation and heat-release rates at four airflows

Test	$\dot{G}_{CO}$, 10^{-2} g/s	$\dot{G}_{CO_2}$, 10^{-1} g/s	$\dot{G}_{SO_2}$, 10^{-2} g/s	$\dot{G}_{H_2S}$, 10^{-3} g/s	$\dot{Q}_A$, kW
		V_o, 0.57 m/s			
4	2.92	5.31	2.94	2.94	5.96
5	2.48	7.79	1.62	2.85	8.61
6	2.95	6.92	1.31	2.46	7.70
Av	2.78	6.67	1.96	2.73	7.43
		V_o, 1.41 m/s			
1	4.84	7.89	4.24	ND	8.89
2	3.50	8.70	6.44	5.16	9.67
3	5.82	7.63	5.99	4.78	8.67
Av	4.72	8.07	5.56	4.97	9.08
		V_o, 2.64 m/s			
7	7.45	8.51	3.40	3.09	9.74
8	9.53	ND	4.18	8.81	ND
9	8.77	13.58	4.77	8.17	15.33
Av	8.59	11.05	4.12	6.69	12.53
		V_o, 3.66 m/s			
10	11.03	16.74	0.39	ND	18.91
11	13.24	14.43	1.46	1.53	16.56
12	13.79	21.78	1.35	.98	24.56
Av	12.69	17.65	1.07	1.26	20.01

ND Not determined.

Table 8.—Flaming coal peak time, heat-release rates, and fire-growth rates at four airflows

Test	t_p, min	Q_i, kW	Q_p, kW	ΔQ, kW	Q_{fg}, kW/min
		V_o, 0.57 m/s			
4	60.0	2.24	6.42	4.17	0.17
5	63.0	3.26	9.76	6.50	.24
6	56.0	2.70	8.36	5.66	.31
Av	59.7	2.74	8.18	5.44	.24
		V_o, 1.41 m/s			
1	52.0	4.35	9.67	5.32	0.25
2	60.0	3.49	11.17	7.69	.31
3	56.0	3.99	9.63	5.64	.27
Av	56.0	3.94	10.16	6.22	.28
		V_o, 2.64 m/s			
7	58.0	3.40	9.49	6.09	0.68
8	69.0	ND	ND	ND	ND
9	57.0	3.41	16.35	12.94	.62
Av	61.3	3.41	14.25	9.51	.65
		V_o, 3.66 m/s			
10	59.0	0.18	19.51	19.33	0.81
11	52.0	.81	15.92	15.11	.86
12	51.0	1.15	20.71	19.57	1.78
Av	54.0	.71	18.72	18.00	1.15

ND Not determined.

Table 9.—Flaming coal smoke characteristics at four airflows

Test	M_o, mg/m^3	N_o, 10^5 p/cm^3	d_m, μm	d_{32}, μm	Obscuration, %	D, m^{-1}	D-CO ratio
			V_o, 0.57 m/s				
4	26.45	10.37	0.354	0.373	34.10	1.811	0.008
5	39.09	10.67	.399	.373	26.69	1.348	.007
6	44.82	11.39	.409	.366	30.82	1.600	.008
Av	36.79	10.81	.387	.371	30.54	1.586	.008
			V_o, 1.41 m/s				
1	27.99	20.28	0.288	0.441	16.03	0.759	0.006
2	30.09	17.62	.309	ND	16.19	.767	.008
3	20.84	15.54	.286	.309	16.49	.783	.005
Av	26.31	17.81	.294	.375	16.24	.770	.006
			V_o, 2.64 m/s				
7	22.30	11.65	0.321	ND	13.59	0.634	0.006
8	29.85	14.88	.327	ND	9.70	.443	.003
9	25.64	12.67	.328	ND	8.72	.396	.003
Av	25.93	13.07	.325	ND	10.67	.491	.004
			V_o, 3.66 m/s				
10	30.12	4.01	0.507	0.290	14.70	0.690	0.006
11	31.03	5.29	.474	.292	10.60	.487	.003
12	25.86	5.12	.444	.247	12.88	.599	.004
Av	29.00	4.73	.475	.276	12.73	.592	.004

ND Not determined.

PRODUCTION CONSTANTS

Table 10 lists the production constants or beta values. They are only calculated for the flaming stage where the fire size is greater, as opposed to the lower concentrations of the smoldering stage. The values for CO_2 remained constant for all air velocities. The β_{CO} tended to increase with velocity but the results for the other beta values show no trend with velocity. Any effect was less evident at the highest velocity where the concentrations were lowest.

The β_{CO} values calculated from a previous report (*9*) are 4.4×10^{-3} g/kJ at an air velocity of 0.37 m/s and 3.6×10^{-3} g/kJ at an air velocity of 0.69 m/s. In a later report (*8*), CO production constants were shown to have the following dependence on air velocity:

$$B_{CO} = 4.8e^{-0.175\ V_o}, \quad (11)$$

where the production constant, B_{CO}, is related to β_{CO} by

$$B_{CO} = 800(\beta_{CO}). \quad (12)$$

The data presented in this report indicate lower values of β_{CO} (or B_{CO}) at low air velocities and higher values of β_{CO} at higher velocities. The discrepancy at the higher velocity (about twice as great as the value in reference 8) should be of little concern, since if under certain conditions, a fire produces more CO, at least the error is toward earlier detection.

At the lower air velocity, the β_{CO} values are lower than those in reference 8 by about 30%. The fact that somewhat lower levels of CO were produced in these tests actually has little impact on the detection aspects of the fire, since at low air velocities and reasonable entry cross-sections the CO alarm level of reference 8 is limited to a maximum value of 10 ppm. It should also be noted that the uncertainty in the individual CO test data is about ±22% of the average value reported.

For smoke optical density, the production constants reported here are lower than those of reference 8 by an average of about 18.4%. The larger discrepancy of about 30.5% occurs at the lowest air velocity. However, for these tests, there is sufficient scatter in the individual test data (about ±25% from the average) that the difference between these data and those of reference 8 are negligible. Also, test conditions such as ignition source, type and quantity of coal, heating rate, and other parameters may have an effect on individual results.

Table 10.—Flaming coal production constants at four airflows

Test	β_{CO}, 10^{-3} g/kJ	β_{CO_2}, 10^{-2} g/kJ	β_{N_o}, 10^{10} p/kJ	β_{M_o}, 10^{-3} g/kJ	β_D, 10^{-2} $(m^2/s)/kW$	β_{SO_2}, 10^{-3} g/kJ	β_{H_2S}, 10^{-4} g/kJ
			V_o, 0.57 m/s				
4	4.90	8.91	1.88	0.48	3.28	4.94	4.93
5	2.88	9.04	1.34	.49	1.69	1.88	3.31
6	3.83	8.98	1.64	.64	2.30	1.70	3.19
Av	3.87	8.98	1.62	.54	2.43	2.84	3.81
			V_o, 1.41 m/s				
1	5.44	8.88	7.02	0.97	2.63	4.77	ND
2	3.62	8.99	5.30	.91	2.31	6.66	5.34
3	6.71	8.80	5.19	.70	2.61	6.90	5.51
Av	5.26	8.89	5.84	.86	2.52	6.11	5.42
			V_o, 2.64 m/s				
7	7.65	8.74	6.91	1.32	3.76	3.49	3.18
8	ND	ND	ND	ND	ND	ND	ND
9	5.73	8.86	4.65	.94	1.45	3.11	5.33
Av	6.69	8.80	5.78	1.13	2.61	3.30	4.25
			V_o, 3.66 m/s				
10	5.83	8.85	1.56	1.18	2.69	0.11	ND
11	8.00	8.72	2.27	1.39	2.18	.89	0.93
12	5.62	8.87	1.54	.78	1.80	.23	.40
Av	6.48	8.81	1.79	1.11	2.22	.41	.66

ND Not determined.

CONCLUSIONS

Under the experimental conditions of this study, increasing the air velocity lengthened the time until the onset of smoldering coal. Cool incoming air forced through the coal pile may have delayed smoldering. During flaming, the greatest impact of air velocity was seen by an increase in the fire-growth rate. As more oxygen was supplied to the fire, its intensity increased at a faster rate.

Concentrations of gas and smoke decreased for both smoldering and flaming coal as the air velocity increased. The emissions were diluted as more air moved through the tunnel. The toxicants found in smaller amounts, SO_2 and H_2S, were reduced to unmeasurable levels at the higher air velocities. The generation rates for CO_2 and CO and the heat-release rate increased during flaming as the air velocity increased. The effects of air velocity on smoldering coal were not as evident due to the lower concentrations of gases produced. However, during smoldering, the generation rates for CO decreased as the air velocity increased from 0.57 to 1.41 m/s. For higher velocities, there was little change. The size of the smoke particles seemed unaffected by these velocities. In this range of velocities and for the size of the coal pile tested, air velocity appeared to have an impact on the gas and smoke produced at the lower velocities. When the velocity was increased above 2.64 m/s, the concentrations of some gases were diluted to levels that were barely measurable. This was due, in part, to the limited amount of coal used in the experiments.

The detectability of a developing fire is affected by the concentration of smoke and CO as well as their transport time. High air velocities speed the transport time of the combustion products, but they also dilute them, possibly below the sensor alarm threshold. This results in either no alarm or slower detector response times. This was true for all the sensor types tested. The lower air velocity produced slightly shorter alarm times than the higher air velocity. Optimum deductibility requires an air velocity that reduces the transport time while still maintaining smoke or CO concentrations above the sensors' alarm threshold. Reducing the time necessary to reach the alarm threshold without sacrificing reliability will increase confidence in the detection system, increasing the possibility of containment or escape while the fire is still in its incipient stage.

REFERENCES

1. Litton, C. D. Diesel-Discriminating Fire Sensor. Paper in Recent Developments in Metal and Nonmetal Mine Fire Protection. BuMines IC 9206, 1988, pp. 28-32.

2. McCaffrey, B. J., and G. Heskestad. A Robust Bidirectional Low-Velocity Probe for Flame and Fire Application. Combust. and Flame, v. 26, No. 1, 1976, pp. 125-127.

3. Patashnick, H., and G. Rupprecht. Microweighing Goes On-Line in Real Time. Res. and Dev., v. 28, No. 6, 1986, pp. 74-78.

4. Cashdollar, K. L., C. K. Lee, and J. M. Singer. Three-Wavelength Light Transmission Technique To Measure Smoke Particle Size and Concentration. Appl. Optics, v. 18, No. 11, 1979, pp. 1763-1769.

5. Tewarson, A. Generation of Heat and Chemical Compounds in Fires. Ch. in The SFPE Handbook of Fire Protection Engineering, ed. by P. E. DiNenno. Natl. Fire Prot. Assoc., 1st ed., 1988, pp. 1-179 to 1-199.

6. Tewarson, A., and J. S. Newman. An Experimental Investigation of the Fire Hazards Associated With Timber Sets in Mines. Paper in Underground Metal and Nonmetal Mine Fire Protection. BuMines IC 8865, 1981, pp. 86-103.

7. Newman, J. S., and J. Steciak. Characterization of Particulates From Diffusion Flames. Combust. and Flame, v. 67, 1987, pp. 55-64.

8. Litton, C. D., C. P. Lazzara, and F. P. Perzak. Fire Detection for Conveyor Belt Entries. BuMines RI 9380, 1991, 23 pp.

9. Egan, M. R. Coal Combustion in a Ventilated Tunnel. BuMines IC 9169, 1987, 13 pp.

APPENDIX.—LIST OF SYMBOLS

D	optical density per unit path length, m^{-1}
d_m	diameter of a particle of average mass, μm
d_{32}	mean particle size, μm
$\dot{G}_X$	generated rate of a given combustion product, g/s or p/s
H_C	net heat of combustion of the fuel, kJ/g
H_{CO}	heat of combustion of CO, kJ/g
I_X	intensity of light, arbitrary units
K_X	theoretical yield of a given gas, g/g
ℓ	optical path length, m
log	logarithm
ln	logarithm, natural
M_X	density of a given gas, $g/(m^3 \cdot ppm)$
M_o	particle mass concentration, mg/cm^3
N_o	particle number concentration, p/cm^3
p	particle
$\dot{Q}_A$	actual heat-release rate, kW
$\dot{Q}_{fg}$	fire-growth rate, kW/min
$\dot{Q}_i$	heat-release rate at ignition, kW
$\dot{Q}_p$	peak heat-release rate, kW
T	transmission of light, %
t_i	time of ignition, min
t_p	time of peak heat-release rate, min
t_s	time of smoldering, min
V_o	air velocity, m/s
V_oA_o	ventilation rate, m^3/s
B_{CO}	CO production constant, $(ppm \cdot m^3)/kJ$
β_X	production constant of a combustion product, g/kJ, p/kJ, and $(m^2/s)/kW$
ΔX	measured change in a given quantity
λ	wavelength of light source, μm
ρ_p	individual particle density, g/cm^3

INT.BU.OF MINES,PGH.,PA 29823

*U.S.G.P.O.: 1993--709-008/80044